Colloid Polym Sci (2017) 295:637–646
DOI 10.1007/s00396-017-4050-8

ORIGINAL CONTRIBUTION

Study on bulk preparation and properties of glycidyl azide polymer with hydroxyl-terminated polyether elastomers obtained through step-wise curing process

Yajin Li[1] · **Song Ma**[1] · **Jingke Deng**[1] · **Yunjun Luo**[1]

Received: 7 November 2016 / Revised: 20 January 2017 / Accepted: 13 February 2017 / Published online: 28 February 2017

Abstract A series of glycidyl azide polymer (GAP) with hydroxyl-terminated poly(ethylene oxide-co-tetrahydrofuran) (P(EO-*co*-THF)) polymer networks of various functional molar ratios (*R*) and different GAP contents have been prepared through the step-wise curing process. The step-wise curing condition is determined based on the thermodynamic parameters of each simplex elastomer system, which is 45 °C-3d then 60 °C-4d. The mechanical properties of the elastomers have been improved from 1.88 to 2.11 MPa in W_{GAP} = 50% under that condition, which is caused by the formation of the larger-sized mesh structure and in consequence the effective elastic strands increase. Meanwhile, the dynamic mechanical analysis (DMA) reveals that the glass transition temperatures of the elastomers are approximately −62.42 and −26.96 °C, respectively. Moreover, it can be concluded through DMA that the P(EO-*co*-THF) domains act as the main crosslinking joints compared with the GAP/N100 domains and thus cause the constrained effect. Combining extension test with DMA results, the network model of the elastomers is depicted. In addition, the thermal stabilities of the blending elastomers have also been studied, and their thermal stabilities meet the requirements of military materials.

Keywords Polymer blends · Step-wise curing · Dynamic mechanical · Polymer networks

Research Highlights:
1. The step-wise curing condition is determined based on the thermodynamic parameters of each simplex elastomer, which is 45 °C-3d then 60 °C-4d.
2. The network structure model is depicted combined extension test with dynamic mechanical analysis.
3. The IPN's network could be obtained through the step-wise curing process, in which the P(EO-*co*-THF)/N100 domains act as crosslinking joints compared to GAP/N100 domains and eventually cause the constrained effect.
4. The blending elastomers have a promising application in military materials.

Electronic supplementary material The online version of this article (doi:10.1007/s00396-017-4050-8) contains supplementary material, which is available to authorized users.

✉ Yunjun Luo
yjluo@bit.edu.cn

[1] School of Materials Science and Engineering, Beijing Institute of Technology, Beijing 100081, China

Introduction

Poly(ethylene oxide-co-tetrahydrofuran) (P(EO-*co*-THF)) polymer has been widely used as a prepolymer for the preparation of nitrate ester polyether (or polyester) (NEPE) propellants. As a typically binder, P(EO-*co*-THF) polymer is getting more and more attention due to its excellent low-temperature mechanical properties since this century [1–3]. P(EO-*co*-THF) polymer belongs to hydroxyl-terminated polyether (HTPE) binders composed of ethylene oxide (EO) and tetrahydrofuran (THF), in which the THF segments offer a superior strength and low-temperature property while the EO segments give rise to a favorable flexibility [4, 5]. However, the P(EO-*co*-THF) polymer is an inert binder, which results in the lower energy for the propellant. Different from P(EO-*co*-THF) polymer, glycidyl azide polymer (GAP) is one of the energetic binders due to the presence of energetic azide groups ($-N_3$) in the polymer chain, which can release energy at ca. 85 kcal/mol [6–8]. Therefore, the incorporation of energetic GAP binder into the inert binder P(EO-*co*-THF) would lead to higher energy by increasing the content of energetic binder without the mechanical property decline.

Meanwhile, polyurethane-based binder systems are extensively used in composite solid propellants due to their convenient reaction conditions [9] and relative lack of adverse side reactions. Commonly, the curing conditions of the blending binder are simultaneous polymerization at the same temperature, which means that both component networks are polymerized concurrently in that process, so this reaction is liable to cause phase separation for the incompatible thermodynamics polymer system. To solve this problem, our team recently reported the sequential polyurethane curation of GAP and HTPB by step-wise curing [10], which proved that the technique of sequential curing is more facile and gives better mechanical properties. In order to further expand the applicability of the step-wise process and improve the GAP/P(EO-*co*-THF) blending elastomers property, we have constructed a facile step-wise curing process for GAP and P(EO-*co*-THF) with polyisocyanate (N100) as the curing agent, as shown in Fig. 1.

In our previous works [11], we reported in situ FTIR kinetic studies of GAP/N100 and P(EO-*co*-THF)/N100, which provided us the kinetic parameters for the curing reaction. Based on the thermodynamic parameters, in this paper, we calculated the relation of conversion rate with time at different temperatures, and then we determined the step-wise process condition, which is 45 °C-3d then 60 °C-4d. The elastomers were successfully prepared under the step-wise curing condition, and the results indicate that the mechanical properties have greatly increased. Furthermore, the network structures were depicted through extension test and dynamic mechanical analysis results. In addition, the thermal gravimetric analyses indicate that the blending elastomers meet the requirements of military materials [8, 12].

Experimental

Materials

The hydroxyl terminated number of GAP polymer was about 29.71 mg KOH/g sample and an average molecular weight was about 3600 g/ml. The hydroxyl terminated number of P(EO-*co*-THF) polymer was about 24.46 mg KOH/g sample and an average molecular weight was about 4038 g/mol. Both the hydroxyl-terminated polymers were purchased from Hubei Aviation Institute of Chemical Technology and purified by vacuum drying.

Desmodur N100 poly-isocyanate had an average molecular weight of 728 g/mol and contained 5.3159 mmol/g of –NCO group, which were taken from Beijing chemical plant.

Taken from Beijing chemical plant, 0.5% dibutyltin dilaurate (DBTDL) (or named T-12) solution in diethyl phthalate (DEP) was used. As well as 0.5% triphenyl bismuth (TPB) solution in dioctyl sebacate (DOS) was taken from Beijing chemical plant.

The aim of the preparation presented in this work is to obtain new series of networks, in which P(EO-*co*-THF)-based polyurethane properties are improved by the GAP binder [11, 13, 14]. The properties in these series have different mechanical and thermal properties, controlled by the compatibility of the polymer blends and the content (wt.%) of GAP.

Measurements

The elastomers were confirmed by ATR-FTIR measurements, and the new absorption peaks appearing at 1731 and 1508 cm^{-1} were assigned to CO and NH stretching due to polyurethane formation. Meanwhile, the NCO stretching band disappeared upon completion of the reaction. The mechanical

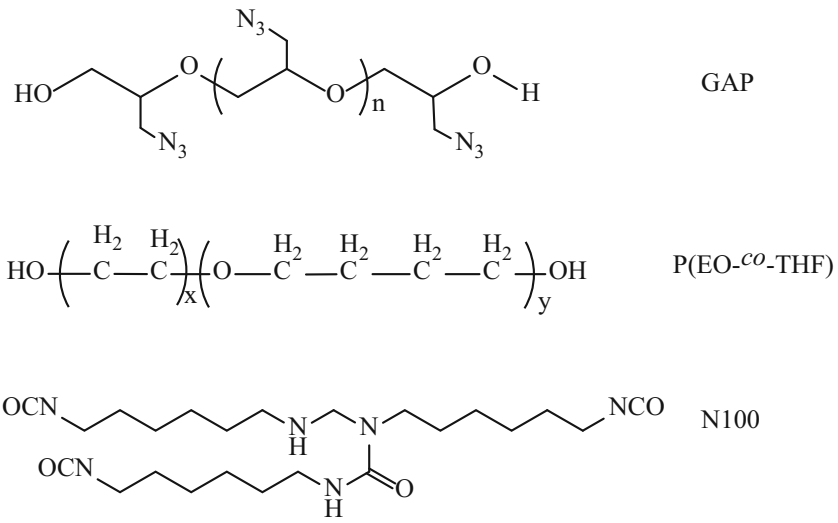

Fig. 1 Structure of GAP, P(EO-*co*-THF), and N100 polymers

properties, including the largest tensile strength (σ_m) and elongation at break (ε_m) of all the dumbbell-shaped specimens, were determined using a universal testing machine (Instron-6022, Shimadzu Co., Ltd.) at a constant rate of 100 mm/min and the results were averaged from five samples.

Dynamic mechanical analysis (DMA) of the elastomers were performed using the METTLER Instrument DMA/SDTA861e at shear model device and a frequency of 1 Hz. The temperature range was from −100 to 100 °C under a nitrogen atmosphere with a heating rate of 3 °C/min. The test specimens were rectangular samples with the length 15 mm, width 5 mm, and thickness 2 mm.

The thermal gravimetric analysis (TGA) was performed on the METTLER Instrument TGA-STAR system at heating rates of 10 °C/min from 30 to 600 °C. The samples of 5 mg were used, and the flow rate of nitrogen gas was 40 mL/min.

Results and discussion

Selection of the curing conditions

In our previous study [11], it was confirmed that hydroxyl-terminated GAP and P(EO-*co*-THF) polymers with polyisocyanate (N100) had different curing mechanisms. Based on the thermodynamic parameters (see Table S6 in Supplementary materials), we calculated the relation of conversion rate with time at different temperatures, then obtained the maximum conversion difference between P(EO-*co*-THF)/N100 and GAP/N100 elastomers under the same temperature and time (Table S1 in Supplementary materials). Based on the fitting curves in Fig. 2, the dependence of the maximum conversion difference with time on temperature is clearly parabolic. Considering the tendency of the minimum duration and conversion difference, we adopt 45 °C-3d as the first curing stage condition, which could reach the maximum conversion difference before phase separation takes place, and 60 °C-4d as the second stage of cure process condition. This step-wise curing process enables the physical entanglement and chemical crosslinking networks to achieve the optimal state for elastomers. Maybe the actual reaction does not completely follow the stage-wise process, but the conversion difference provides a theoretical basis for GAP and P(EO-*co*-THF) blending elastomers.

Static mechanical properties

Adopting the simultaneous and step-wise curing conditions for GAP/P(EO-*co*-THF) blends, elastomers of GAP/P(EO-*co*-THF) with various mole equivalent ratios (R values) have been prepared using polyisocyanate (N100) as the curing agent, and their mechanical properties are listed in Fig. 3 (Table S2 in Supplementary materials). The stresses σ_m and elastomer modulus E of simultaneous curing elastomers increase from 1.23 and 0.58 × 10^{-2} MPa to 1.88 and 1.84 × 10^{-2} MPa, respectively; while the σ_m and E of step-wise curing elastomers increase from 1.38 and 0.62 × 10^{-2} MPa to 2.11 and 2.42 × 10^{-2} MPa, respectively. In contrast, the strain ε_m of simultaneous and step-wise elastomers decrease from 211.68 and 222.11% to 102 and 87.21%, respectively. The curves of σ_m and ε_m including E for elastomers are shown in Fig. 3. The dependence of the elastomer mechanical properties on R is clearly presented, and through Fig. 3, we can see that the change of curing conditions improves the mechanical properties. Through comprehensively considering the

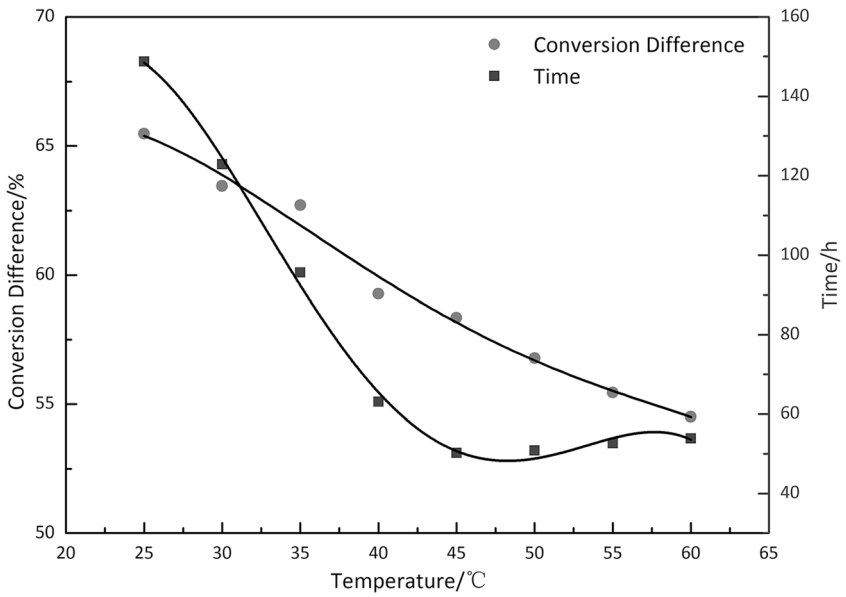

Fig. 2 Dependences of conversion difference with time on same temperature for elastomers

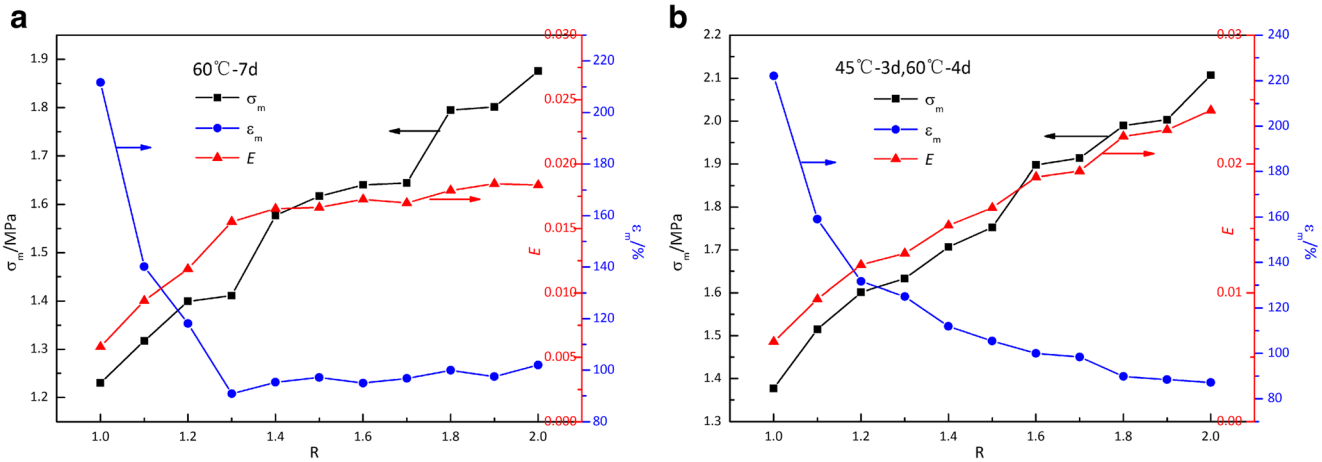

Fig. 3 Effect of R value (the molar ratio of [NCO]/[OH]) on the σ_m, ε_m, and E of GAP/P(EO-*co*-THF) elastomers. (50% content of GAP) (**a**). Conventional one-step curing (60 °C-7d) (**b**). Step-wise curing process (45 °C-3d, 60 °C-4d)

experiment results, we can conclude that the R value of 1.3 has optimal mechanical properties with tensile strength of 1.63 MPa and breaking elongation of 125%.

On account of the above results, we chose R value of 1.3 to study effects of GAP content on mechanical properties. Based on the compatibility of the polymer at specific concentration levels [15], we prepared GAP-based elastomers at different relative weight ratios, and their mechanical properties are listed in Fig. 4 (Table S3 in Supplementary materials). For elastomers prepared by simultaneous curing process with GAP content less than 50%, the σ_m of the blend increases from 1.43 to 1.53 MPa, then decreases to 0.82 MPa, and the ε_m increases from 72.2 to 131.2%. Meanwhile, the E decreases from 1.98×10^{-2} to 0.67×10^{-2} MPa due to the decrease of the crosslinking density along with the increase in W_{GAP}. In comparison, as the step-wise curing process of GAP/P(EO-*co*-THF), elastomers has enough space to form crosslink networks before phase separation happens, the σ_m of the blend increases from 1.49 to 1.57 MPa, then decreases to 0.71 MPa, and the ε_m increases from 110.7 to 169.1% at less than 50% GAP content, then decreases to 149.1% after 60% GAP content. This phenomenon shows that the step-wise curing condition effectively improves the mechanical properties in $W_{GAP} \leq 0.5$, and probably the blending elastomers form partial miscibility macromolecule alloy structures such as island structure, layered structure and interpenetrating structure [16]. This result is fully consistent with the dynamic mechanical analysis as well (see Figs. 7 and 8).

Dynamic mechanical analysis

The tan δ responses of GAP/N100 and P(EO-*co*-THF)/N100 elastomers measured by DMA are shown in Figs. 5 and 6. The elastomers have damping peaks at approximately −62.42 and −26.96 °C, respectively, corresponding to the glass transition of

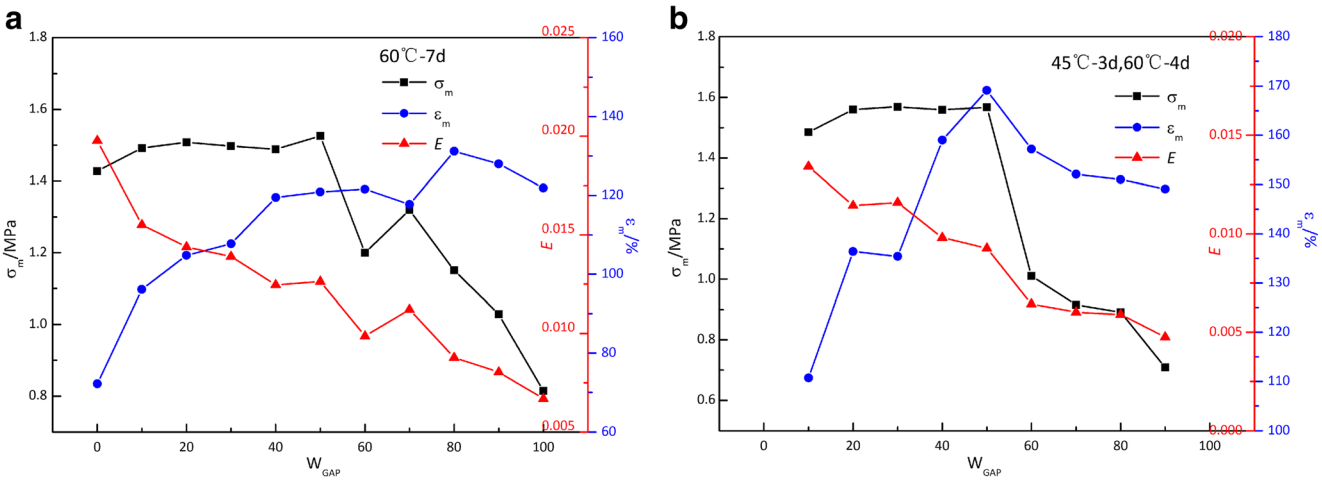

Fig. 4 Effect of weight percentage of GAP on the σ_m, ε_m, and E of GAP/P(EO-*co*-THF) elastomers (R is 1.3). Conventional one-step curing (60 °C-7d) (**a**). Step-wise curing process (45 °C-3d, 60 °C-4d) (**b**)

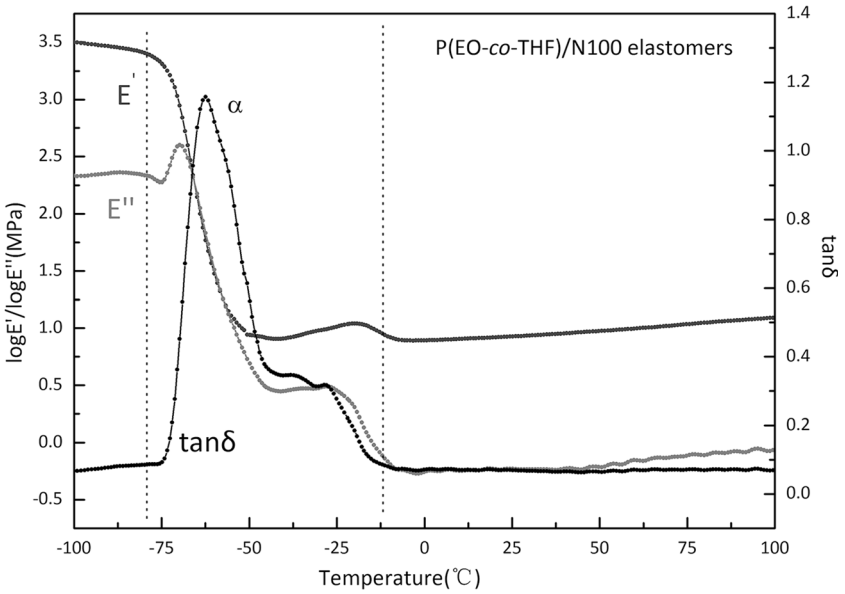

Fig. 5 DMA curves of P(EO-*co*-THF)/N100 elastomer

the copolyether strands [17]. The GAP/N100 elastomers display a faint relaxation at low temperature, which can be attributed to β relaxation. This relaxation is centered around −75 °C and may be associated with the movement of the pendant group $(-CH_2N_3)_n$ segments [18]. Furthermore, P(EO-*co*-THF)/N100 elastomers have one plateau-raising peak at approximately −23 °C, because of the crystallization and melting process for P(EO-*co*-THF) chains. At the region of glass transition, the P(EO-*co*-THF)/N100 elastomers have a broader peak shape and lower tan δ value than GAP/N100 elastomers, which indicates that the dynamic performance for P(EO-*co*-THF)/N100 elastomers is weak, but P(EO-*co*-THF)/N100 elastomers have excellent impact toughness at low temperature due to the high E'.

In a polymer blend, the components can result in homogeneous phase or phase separation according to the thermodynamic properties for GAP/P(EO-*co*-THF) elastomers. In order to avoid too many overlapping data, the variations of the main viscoelastic parameters (E', E'', tan δ) with temperature for the considered samples are depicted in three separated figures, and the E' and E'' are valued with logarithmic form for the sake of clarity. Figure 7 exhibits the variation of tan δ with temperature for different GAP contents of GAP/P(EO-*co*-THF) elastomers, and the corresponding experimental data are listed in Table S4 in Supplementary Materials. The GAP/P(EO-*co*-THF) system displays phase separation when $W_{GAP} \geq 0.3$ and $W_{GAP} \leq 0.9$, and there are two noticeable regions in the tan δ curves. Interestingly,

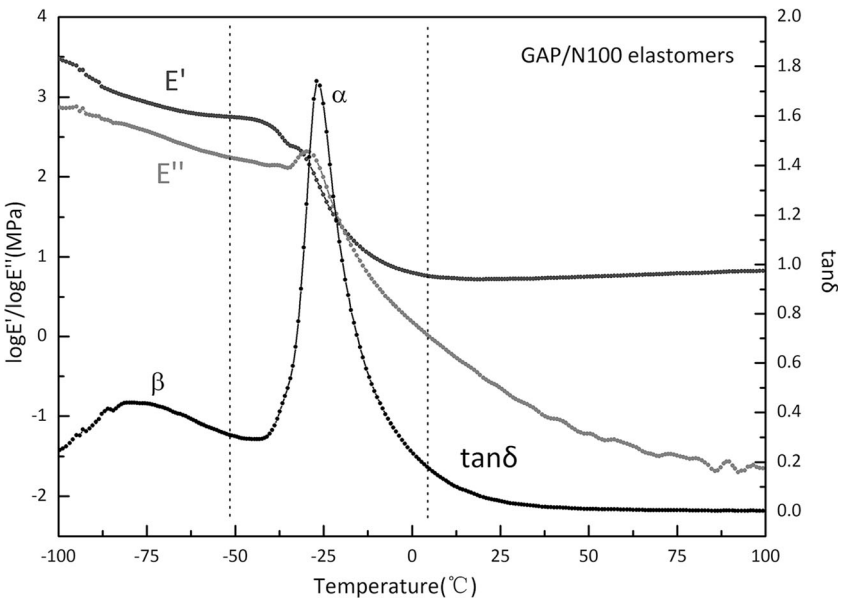

Fig. 6 DMA curves of GAP/N100 elastomer

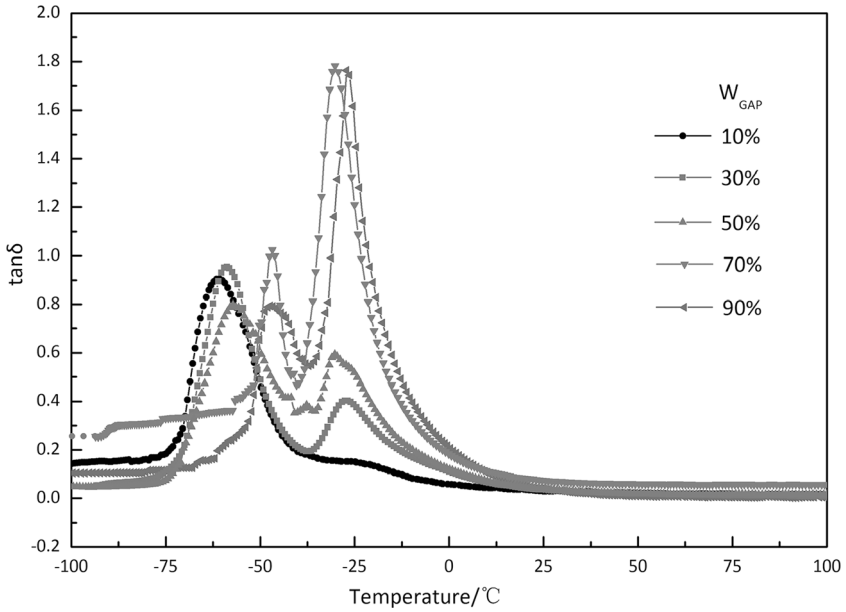

Fig. 7 Dependences of tan δ on temperature with wt.% GAP

$T_{\alpha,1}$ and $T_{\alpha,2}$ are gradually approaching with the increase of GAP content, and such a behavior may be due to the island or interpenetrating structure formation between the chains, which superimposes additional physical network to the existing chemical network. That is to say, when the linear chains (P(EO-*co*-THF)) act as the main part of the blends, the most visible changes in the dynamic mechanical behavior are the increase of the tan δ peak value, simultaneously with a slight peak shift to lower temperature (Fig. 7, Table S4 in Supplementary materials). The P(EO-*co*-THF)/N100 sample is partially crystalline (the melting temperature is about −8 °C), but the similar phenomenon is not visible for the blending elastomers in the tan δ curves because of the chain rigidity improvement.

Figures 8 and 9 exhibit the variations of E' and E'' with temperatures for the different GAP contents of elastomers. The E'' peak appears always at a lower temperature than tan δ peak [19, 20]. The onset of the main α relaxation starts over the temperature of −65 °C and spans till 40 °C. There are some peculiar characteristics of this relaxation, for example, the E' values in this range exceed 10^9 Pa, which is specific for the blending elastomers in the glassy state. The fall of E' in glass transition region is smooth and large and the second plateau value of the E' is over 10^7 Pa when $W_{GAP} \leq 0.5$, meanwhile they all have two weak shoulders on E''. This means a decrease of E' with about two orders of magnitude in this transition region. The low tan δ peak value together with the E'

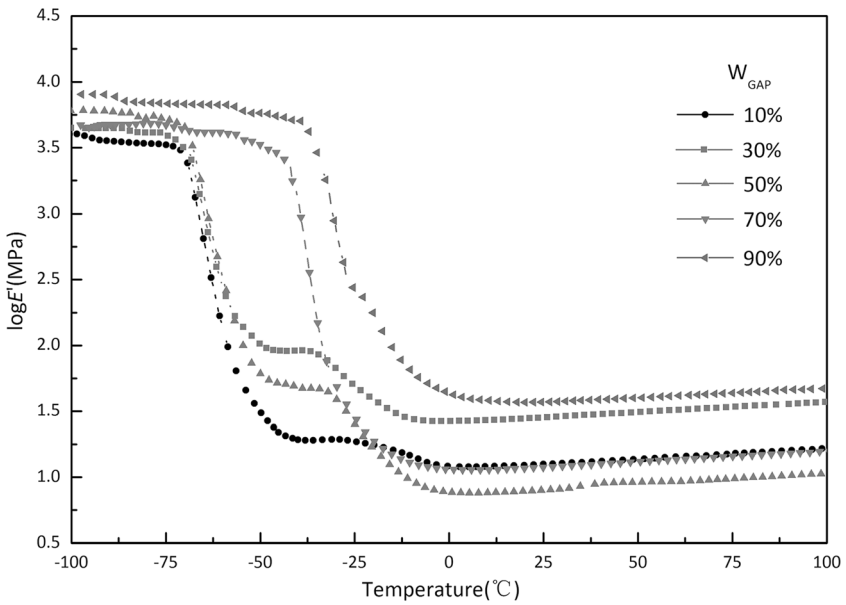

Fig. 8 Dependences of storage modules on temperature with wt.% GAP (step-wise curing process (45 °C-3d, 60 °C-4d))

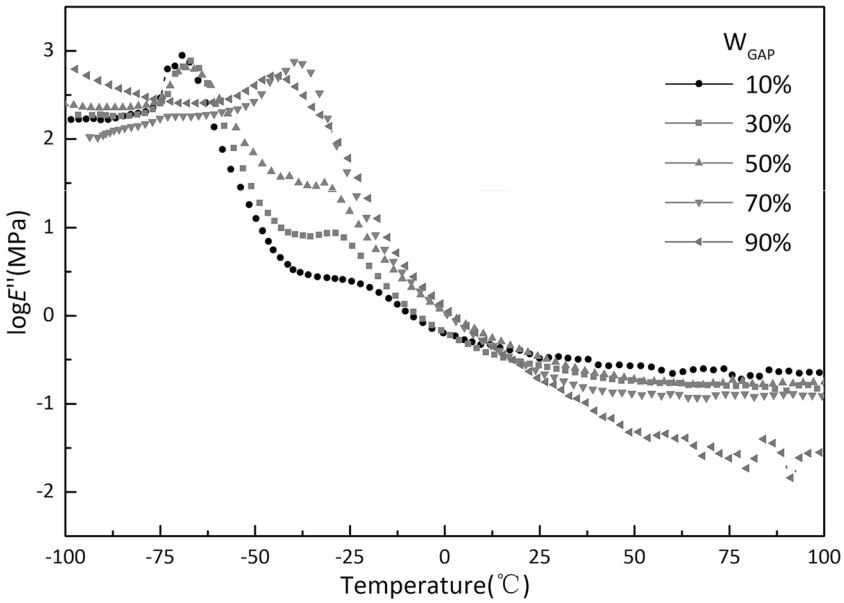

Fig. 9 Dependences of loss modules on temperature with wt.% GAP (step-wise curing process (45 °C-3d, 60 °C-4d))

decrease of two orders of magnitude indicate the presence of some movement restraints in the soft domains such as interlocking and entanglement networks [21]. When $W_{GAP} \leq 0.5$, the large E'' peak situated around −70 °C is followed by a downturn after −60 °C, a clear sign of flowing. Followed the trend of E'' curve it is obvious that this flowing is slowed down after −40 °C and almost stopped after −25 °C. All the transformations can be attributed to the hard phase of GAP chains being embedded in the P(EO-*co*-THF) soft network. The narrow tan δ peak shape and E' rise are the characteristic of the homogeneity of the network, which is formed before $W_{GAP} \leq 0.5$. When $W_{GAP} > 0.5$ in the elastomers, the E' and E'' only have one variation tendency due to the GAP chain movement. As expected, P(EO-*co*-THF)/N100 domains act as crosslinking joints compared to GAP/N100 domains and eventually cause this constrained effect.

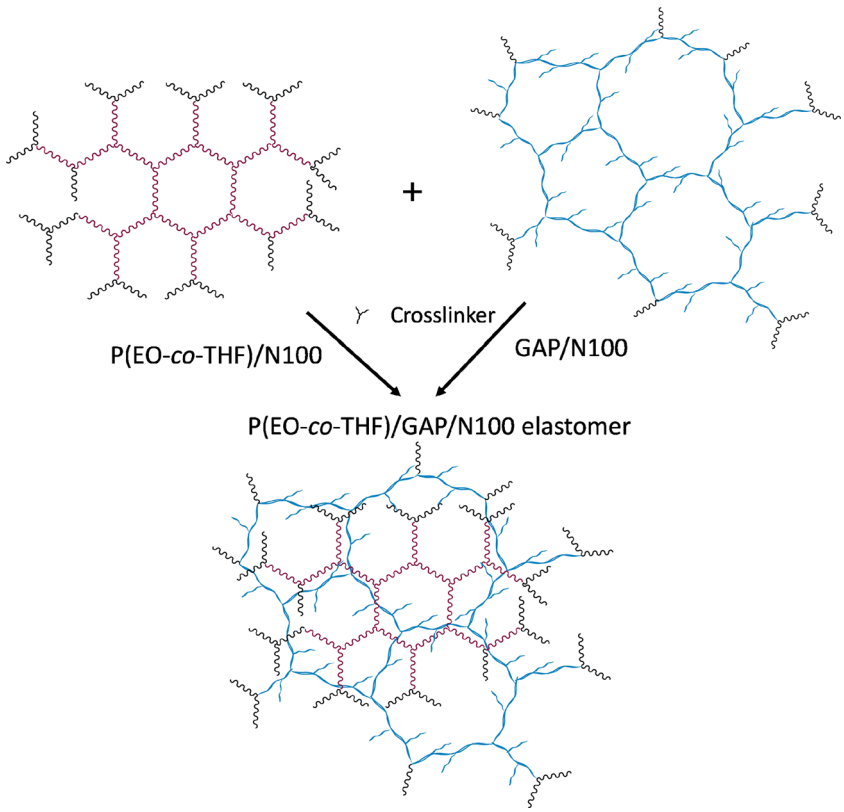

Fig. 10 Network model of elastomers for P(EO-*co*-THF)/N100, GAP/N100, and blending networks P(EO-*co*-THF)/GAP/N100

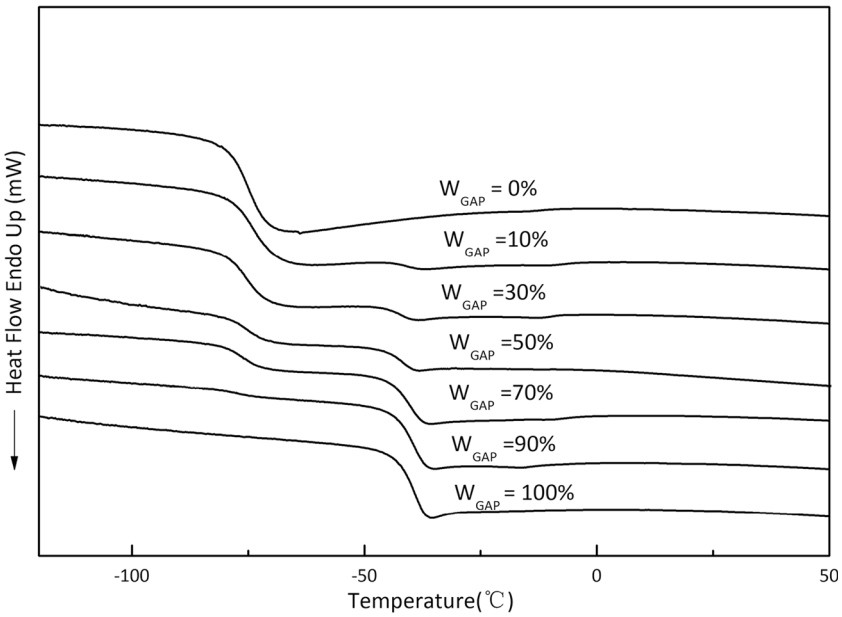

Fig. 11 DSC curves for blending elastomers with various contents of GAP (step-wise curing process (45 °C-3d, 60 °C-4d))

Network model

If we ignore the side-reaction of polyurethane such as the formation of allophanate [22, 23], the network structure model of elastomers can be established in Fig. 10. For the reason that the curing agent (N100) is three functional groups, N100 is not only the crosslinking agent but also the chain extender. The resulting network structure is comprised of three-dimensional networks, and nearly all terminal groups are –NCO for elastomers ($R > 1.0$). For GAP/N100 elastomers, there are many $-CH_2N_3$ dangling strands in the networks, causing the formation of larger-sized mesh and finally resulting in effective elastic strands increase. Conversely, P(EO-*co*-THF)/N100 network plays the role of chain extension and is crucial to the geometric network strength. With the formation of crosslinking points, the physical entanglement and hydrogen bond effect also improve the network properties because of the intermolecular force.

Based on the network model, it can be concluded that the GAP/P(EO-*co*-THF) blending elastomers have excellent mechanical properties in a certain proportion of GAP because of its compatibility; however, both the binders are not miscible and phase separation occurs for a while after dispersion [15]. The aim of the step-wise curing process is to cure completely before phase separation occurs.

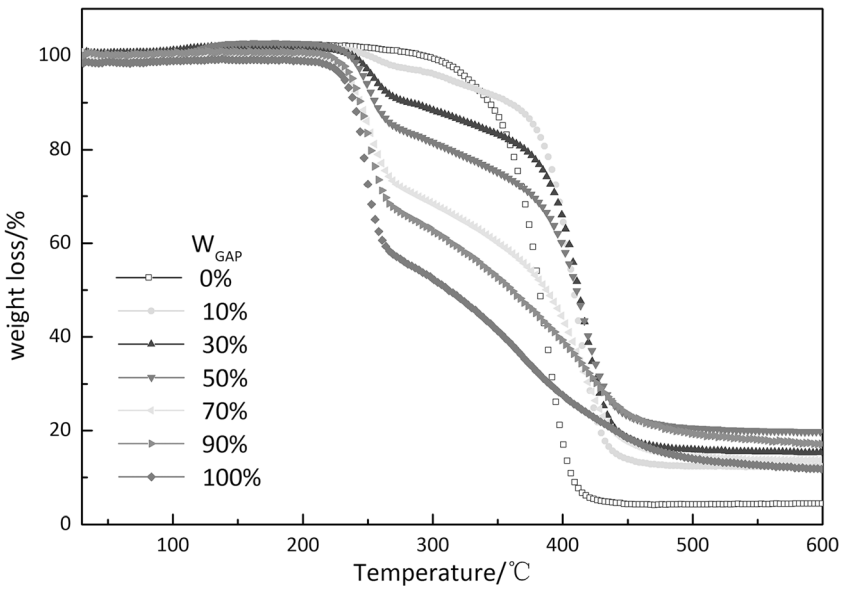

Fig. 12 TG curves for blending elastomers with various contents of GAP (step-wise curing process (45 °C-3d, 60 °C-4d))

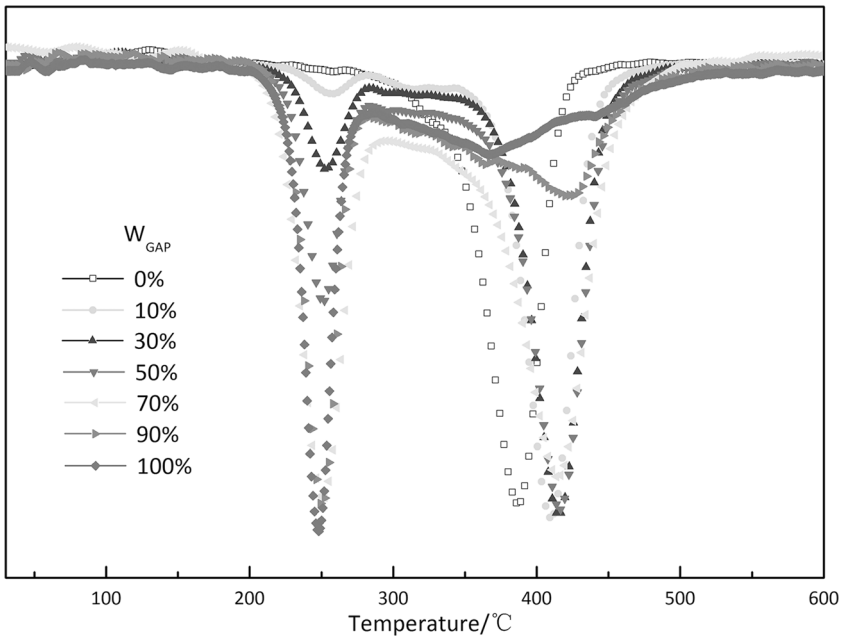

Fig. 13 DTG curves for blending elastomers with various contents of GAP (step-wise curing process (45 °C-3d, 60 °C-4d))

Differential scanning calorimetry (DSC) analysis

Figure 11 shows the DSC thermograms of blending elastomers with different weight ratios. The glass transition temperatures (*Tg*) of the pure P(EO-*co*-THF) and GAP networks are found to be −80 and −42 °C, respectively. With the increase in weight ratios of GAP, the DSC thermograms show two glass transition temperatures, which are located in between pure GAP and P(EO-*co*-THF) polymers, respectively. This phenomenon may be the result of microphase separation but fortunately the mechanical properties are enhanced. The copolymer networks form a polymer alloy, including physical entanglements and interlocking of polymer networks and reduction of gap between cross-linked points.

Thermal stability

To assess the thermal stabilities of the blending elastomers, thermal gravimetric analyses of different GAP content elastomers have been performed, and the thermogravimetric (TG) and derivative thermogravimetric (DTG) curves are shown in Figs. 12 and 13.

As shown in Fig. 12, the thermal weight losses start after 230 °C and finish before 460 °C, and the accompanying weight losses are listed in Table 5 (Table S5 in Supplementary materials). Meanwhile, the DTG curves present three peaks, which indicates that the elastomers have three decomposition stages. The thermal cleavage temperatures of the azide groups are nearly 230 ~ 255 °C; the decomposition temperatures for the hard segments are nearly 255 ~ 400 °C; the last stage is corresponding to the copolyether strands' decomposition of about 400 ~ 460 °C. Hence, the blending elastomers that are crosslinked by GAP and P(EO-*co*-THF) polyether have a higher thermal stability, which can be used as a promising military material.

Conclusions

Step-wise curing process (45 °C-3d; 60 °C-4d) has been determined through the thermodynamic parameters of the elastomer formation. In comparison with conventional one-step curing condition, step-wise curing process has effectively improved the elastomer properties because it forms macromolecule alloy structures such as island structure, layered structure, and interpenetrating structure.

The elastomers with various functional molar ratios (*R*) and different contents of GAP have been successfully prepared using the step-wise curing process. The mechanical properties of the elastomers have been improved in $W_{GAP} \leq 0.5$ under the step-wise condition, and there are many $-CH_2N_3$ dangling strands in the GAP-based networks, causing the formation of larger-sized mesh and finally resulting in effective elastic strands increase. Meanwhile, the dynamic mechanical properties prove that P(EO-*co*-THF)/N100 domains act as crosslinking joints for GAP/N100 domains and cause the constrained effect. The weight losses of the GAP/P(EO-*co*-THF) elastomers are characteristic of the three-step decomposition, and the thermal stabilities meet the requirements of military materials [8, 12].

Acknowledgements This work was supported by the National Natural Science Foundation of China (NSFC) [U1630142].

Compliance with ethical standards

Conflict of interest The authors declare that they have no conflict of interest.

References

1. Li S, Liu Y, Tuo X, Wang X (2008) Mesoscale dynamic simulation on phase separation between plasticizer and binder in NEPE propellants. Polymer 49(11):2775–2780
2. Yang Y, Y-j LUO, J-r L, Ge Z (2008) Effect of Trifuntional PET on the mechanical properties of elastomer and NEPE propellant [J]. Fine Chem 2:005
3. Kanti Sikder A, Reddy S (2013) Review on energetic thermoplastic elastomers (ETPEs) for military science. Propellants Explos Pyrotech 38(1):14–28
4. Comfort T, Dillman L, Hartman K, Mangum M, Steckman R Insensitive HTPE propellants. In: Proceedings of the JANNAF Propulsion Meeting, 1996. CPIA Publication 630, p 87
5. Fisher Michael J (2004) HTPE propellants mature over last decade. Johns Hopkins Univ Chem Propulsion Inf Agency 2:4–5
6. Selim K, Özkar S, Yilmaz L (2000) Thermal characterization of glycidyl azide polymer (GAP) and GAP-based binders for composite propellants. J Appl Polym Sci 77(3):538–546
7. Nazare A, Asthana S, Singh H (1992) Glycidyl azide polymer (GAP)—an energetic component of advanced solid rocket propellants—a review. J Energ Mater 10(1):43–63
8. Bhowmik D, Sadavarte VS, Pande SM, Saraswat BS (2015) An energetic binder for the formulation of advanced solid rocket propellants. Central Eur J Energ Mater 12(1):145–158
9. Flory PJ (1953) Principles of polymer chemistry. Cornell University Press.
10. Tanver A, Rehman F, Wazir A, Khalid S, Ma S, Li X, Luo Y, Huang M-H (2016) Energetic hybrid polymer network (EHPN) through facile sequential polyurethane curation based on the reactivity differences between glycidyl azide polymer and hydroxyl terminated polybutadiene. RSC Adv 6(13):11032–11039
11. Li Y, Li J, Ma S, Luo Y (2016) Different catalytic systems on hydroxyl-terminated GAP and PET with poly-isocyanate: curing kinetics study using dynamic in situ IR spectroscopy. International Journal of Polymer Analysis and Characterization:1–9
12. DeLuca LT (2017) Highlights of solid rocket propulsion history. In: Chemical rocket propulsion. Springer, 1015–1032
13. Wang X, Luo Y, Wang X, Ge Z (2010) Properties of GAP/PET dual-soft segments energetic polyurethane elastomer. CIESC J 3:038
14. Zhen WXLYG, Kai G (2009) Study on properties of GAP/PET polyurethane binder films [J]. New Chem Mater 12:027
15. Porter RS, Wang L-H (1992) Compatibility and transesterification in binary polymer blends. Polymer 33(10):2019–2030
16. Hisamatsu T, Nakano S, Adachi T, Ishikawa M, Iwakura K (2000) The effect of compatibility on toughness of PPS/SEBS polymer alloy. Polymer 41(13):4803–4809
17. Zhang B, Tan H (1998) Studies of novel segmented copolyether polyurethanes. Eur Polym J 34(3):571–575
18. Pukánszky B, Bagdi K, Tóvölgyi Z, Varga J, Botz L, Hudak S, Dóczi T (2008) Nanophase separation in segmented polyurethane elastomers: effect of specific interactions on structure and properties. Eur Polym J 44(8):2431–2438
19. Okrasa L, Czech P, Boiteux G, Mechin F, Ulanski J (2008) Molecular dynamics in polyester—or polyether-urethane networks based on different diisocyanates. Polymer 49(11):2662–2668
20. Mondal S, Hu J (2008) Structural characterization and mass transfer properties of dense segmented polyurethane membrane: influence of hard segment and soft segment crystal melting temperature. Polym Eng Sci 48(2):233–239
21. Cristea M, Ibanescu S, Cascaval CN, Rosu D (2009) Dynamic mechanical analysis of polyurethane-epoxy interpenetrating polymer networks. High Perform Polym 21(5): 608–623
22. Mcelroy WR (1967) Preparing polyurethanes. US Patents: 1967
23. Ullrich M, Meisert E, Eitel A (1976) Process for the production of polyurethane elastomers. US Patents: 3963679, 1976